MULTIPLE QUANTUM SPECTRUM OF ORIENTED HEXANE-d_6

G. DROBNY [1], D.P. WEITEKAMP [2] and A. PINES

*Department of Chemistry, University of California, Berkeley
and Materials and Molecular Research Division, Lawrence Berkeley Laboratory, Berkeley, CA 94720, USA*

The proton multiple quantum NMR (MQ NMR) spectrum of methyl-deuterated hexane-d_6 is obtained in a nematic solvent. Rough simulation of the six- and seven-quantum spectra is achieved with a simple model of conformer probabilities and ordering. The advantages and prospects of MQ NMR for the conformational analysis of ordered, non-rigid molecules are discussed.

1. Introduction

1.1. NMR of non-rigid molecules in anisotropic phases

The conformation and ordering of polymethylene chains is an important problem in the theory of liquids, liquid crystals and polymers. In the liquid crystalline phases these questions are sometimes amenable to study by NMR. The anisotropy of the molecular ordering leads to measureable values for the motionally averaged second-rank tensors characterizing the electric quadrupole and dipole–dipole couplings [1]. The rapid molecular diffusion averages away intermolecular spin couplings thus allowing a treatment in terms of single molecule spectra.

The bulk of the work in this area has employed deuterium NMR of isotopically labelled molecules [2–7]. The advantage of this approach is that the quadrupole satellites are often resolved and assignable to unique chain positions giving a local measure of order. The disadvantage is that the relatively small magnetogyric ratio and short relaxation times of deuterium allow little or no

resolution of the finer structure due to the direct dipole interaction between spins.

These dipole interactions are essential to obtaining the fullest possible picture of molecular structure in liquid crystals. To appreciate this, consider the form of the quadrupole and dipole couplings which determine the high-field spectra:

$$\nu_i^Q = \left[eQ_iV_i^{33}/4I(2I-1)h \right] \langle \tfrac{1}{2}(3\cos^2\theta_i - 1)\rangle, \tag{1}$$

$$D_{ij} = -\left(h\gamma_i\gamma_j/4\pi^2 \right)\langle \tfrac{1}{2}(3\cos^2\theta_{ij} - 1)/r_{ij}^3\rangle. \tag{2}$$

The quadrupole coupling has been written for the axially symmetric case, which is appropriate for sp^3 C–D bonds. The bracketed function describes time averaging of the angle between the bond and the field direction and contains the information of interest. The dipole coupling of (2) is an even richer source of averaged molecular geometry. The constants are known and the dependence on the configuration enters not only through the angle of the internuclear vector but also through its length r_{ij}.

The most crucial difference between (1) and (2) is that the quadrupole couplings are single particle properties while the dipole couplings are pair properties. The former increase linearly with the number of spins while the latter increase quadratically. This quadratic increase in information con-

tent is needed to keep pace with the increase in the number of unknowns as the chain lengthens. The complexity comes from the fact that the observables are weighted averages of rapidly interconverting conformers. Thus for the dipolar couplings

$$D_{ij} = \sum_n P_n D_{ij}^n, \qquad (3)$$

where P_n is the probability of the nth conformers and D_{ij}^n is the average coupling between spins i and j in that particular conformation. Such an expansion in a finite number of conformers is an application of the rotational isomeric state model of Flory [8] and has been widely used in interpreting deuterium NMR of polymethylene systems [2–7,9,10]. The conditional dipolar couplings, appearing on the rhs of (3), are related for the different internuclear pairs. This can be seen by expressing them in a common molecule fixed frame [1,9,11]:

$$D_{ij}^n = -\left(h\gamma_i\gamma_j/4\pi^2\right)$$
$$\times \sum_{r=-2}^{2} \frac{D_{0r}^{(2)}\left(\Omega_0^{ijn}\right)}{r_{ijn}^3} C_{-r0}^{(2)}(\Omega_1^n)(-1)^{-r}. \quad (4)$$

The second-rank Wigner rotation matrix elements $D_{0r}^{(2)}$ depend only on internal geometry of the conformer. The $C_{-r0}^{(2)}$ describe the external degrees of freedom consisting of the orientation of the molecular frame with respect to the coincident director and magnetic field directions.

Further progress can be made with the expansion (4) if the implicit motional averaging is assumed to be separable for the internal and external coordinates, as has been discussed from several viewpoints [1,9,12]. This separation is warranted if the vibrational motion is negligible around the local minima in the potential corresponding to the various conformers, or if this motion is independent of molecular orientation. Then the $C_{-r0}^{(2)}(\Omega_1^n)$ are the complex form of Saupe's order tensor [13] $\mathbf{S}^n$ with the superscript indicating the possibility of a different order tensor being necessary for each conformer. If the internal geometry of each conformer is taken as adequately known, then the remaining unknowns are of the form $P_n\mathbf{S}^n$; i.e.

probabilities multiplied by order tensors [14].

For polymethylene chains the conformers are enumerated by recognizing that there are three local minima in potential energy as each C–C bond is rotated. The lowest energy form is the trans (t) and the two equivalent higher energy minima are the gauche (g$^\pm$) forms located about $\pm120°$ away. Extension of the chain by one methylene unit triples the number of configurations. The number of single particle interactions, such as deuterium quadrupole couplings, increases only linearly with chain length and is never sufficient. The dipolar interactions on the other hand will often be sufficient in number to allow inversion of (3) and (4) to solve for the unknowns and, in any case, they provide a much fuller picture. The example of n-hexane is discussed in section 2.

1.2. Multiple quantum NMR

The measurement of the D_{ij} needed to model the unknowns $P_n\mathbf{S}^n$ is impeded by a fundamental difficulty. One would like to measure the proton NMR spectrum, since the large gyromagnetic ratio leads to sizeable couplings even for spins several segments apart. However, for systems of more than a few protons, spectral congestions rapidly leads to a loss of resolved structure. Even when some lines remain resolved, their great density introduces considerable uncertainty in the assignment of transitions to the energy level diagram, which is an explicit or implicit step in any spectral simulation scheme.

These problems may be described as a mismatch between the measured quantity, the single quantum spectrum, and its information content. The number of single quantum transitions for N dipolar coupled protons is $(2N)!/(N+1)!(N-1)!$ in the absence of permutation symmetry. On the other hand there are at most $N(N-1)/2$ unique couplings D_{ij}. Thus the complexity of a single quantum spectrum is an unfortunate impediment to solving the simpler underlying problem.

A solution to this dilemma has been found in the use of proton Fourier transform multiple quantum NMR (MQ NMR) in liquid crystalline solvents [15–18]. This technique allows the recording of the far simpler spectra corresponding to the

simultaneous absorption of n photons from the Larmor-frequency radiation field. For example, the number of transitions in which $n = N - 2$ of the N protons flip is only $N(2N - 1)$. This is of the same order as the number of dipolar couplings to be measured. Proton MQ NMR in liquid crystals has been applied already to two much simpler non-rigid systems. The azimuthal angles of the two methyl groups of 2,3-dimethylmaleic anhydride in a nematic solvent were shown to be uncorrelated on the NMR timescale [17]. The dihedral angle of 4-cyano-4'-n-pentyl-biphenyl was estimated to be $\approx 32°$ in the nematic phase [18]. Neither of these cases involved unknown conformational probabilities. Refs. [19,20] review MQ NMR, including applications in liquid crystals.

2. n-hexane-d_6 in a nematic solvent

2.1. Experimental

The sample consists of 55 mg of n-hexane-1,1,1,6,6,6-d_6 (n-hexane-d_6) dissolved in 300 mg of p-octylphenyl-s-chloro-4(p-heptylbenzoyloxy)benzoate (Eastman 15230). The spectra are recorded in the nematic phase at $33 \pm 0.1°C$. The proton Larmor frequency is 185 MHz. The coil is double resonant to allow deuterium decoupling throughout. Proton 90° pulse times are 3 μs.

The pulse sequence for the single quantum spectrum is $90-t_1/2-180-t_1/2$-sample. The Hahn echo amplitude [21] as a function of t_1 is Fourier transformed to give the homogeneous spectrum. For the multiple quantum experiment, the pulse sequence $90-\tau-90-t_1/2-180-t_1/2-90-\tau$-sample shown in fig. 1 is used with time proportional phase increments (TPPI) of the preparation pulses as described earlier [16]. This gives a homogeneous multiple quantum spectrum of all orders n.

2.2. Results

The number of transitions expected in each multiple quantum order of a polymethylene chain may be calculated by group theoretical methods. Let us assume that the chain rapidly interconverts between conformers and that the symmetry of the
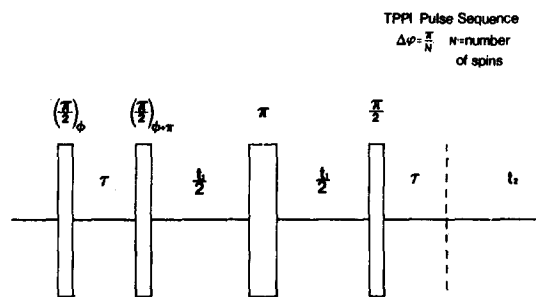

Fig. 1. The four-pulse multiple quantum experiment includes a 180° pulse in the middle of the evolution period to refocus dephasing due to magnetic field inhomogeneity. To effect a n-dependent separation of multiple quantum transitions, the phases of the first two pulses are incremented by $\Delta\phi = \pi/N$ with Δt_1. N is the number of spin 1/2 nuclei.

motion is two-fold in the sense that for a given bond, a t to g^+ rotation occurs with equal probability to a t to g^-. Furthermore, if the ends of the chain are indistinguishable, the NMR permutation group is isomorphic to C_{2h}. Now the character table may be expressed, in reducible form using a direct product basis for the eight protons of a four-methylene chain. A decomposition of each reducible representation into irreducible components yields the energy level diagram, which is shown in table 1. From the energy level diagram the number of transitions in each multiple quantum order may be easily obtained, and are shown in table 2. Note that 2860 lines will occur in the single quantum region whereas merely two pairs of lines will occur in the seven-quantum region and fourteen pairs will occur in the six-quantum region. In addition an eight-fold degenerate central

Table 1
n-hexane-d_6. Energy level density

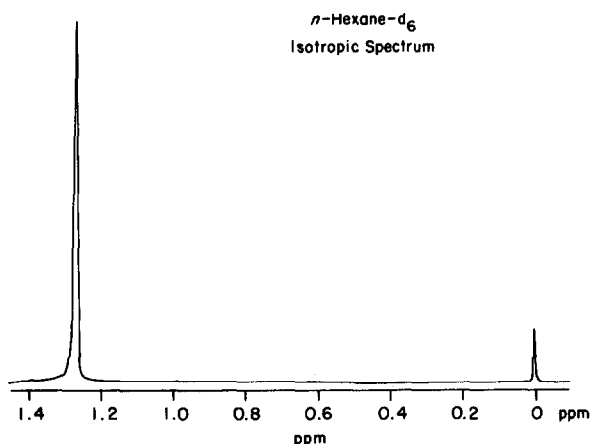| m	A_g	A_u	B_g	B_u
4	1			
3	2	2	2	2
2	10	6	6	6
1	14	14	14	14
0	22	16	16	16
−1	14	14	14	4
−2	10	6	6	6
−3	2	2	2	2
−4	1			

Fig. 2. The isotropic high-resolution proton spectrum of methyl-deuterated n-hexane. The line at 0 ppm is TMS.

Table 2
Number of n-quantum transition ($\Delta m = n$)

Δm	
8	1 line at 8 $\Delta\omega$
7	2 pairs
6	14 pairs
5	70 pairs
4	224 pairs
3ı	546 pairs
2	944 pairs
1	1430 pairs
0	1049 pairs

line will occur at the center of the six-quantum region, but is uninteresting since its frequency is independent of dipolar couplings.

Fig. 2 shows the high-resolution proton NMR spectrum of n-hexane-d_6 in isotropic solution obtained with deuterium decoupling. The single line at 2 ppm indicates a negligible difference between

the isotropic chemical shifts of protons on inequivalent methylene groups, and so no information on chain configuration may be obtained from the isotropic spectrum. The line at 0 ppm is from TMS.

In fig. 3 is shown the spin echo single quantum spectrum of the eight methylene protons of partially oriented n-hexane-d_6. No attempt is made to analyze this spectrum.

Fig. 4 is the result of the four-pulse multiple quantum sequence applied to the same sample of n-hexane-d_6. To obtain this spectrum, fifteen dis-

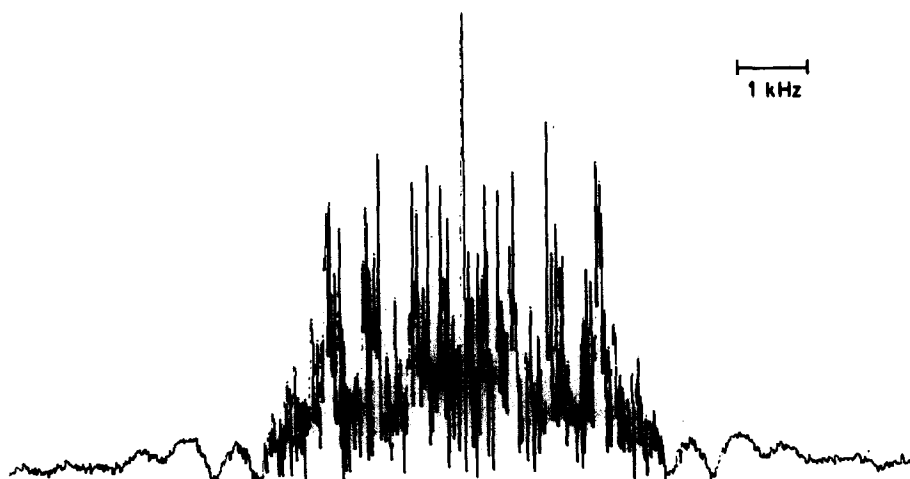Oriented n-Hexane-d_6
Single Quantum Spectrum

Fig. 3. The single quantum spin echo proton spectrum of oriented methyl-deuterated n-hexane. Group theoretical calculations predict 2860 transitions.

n-Hexane-d_6
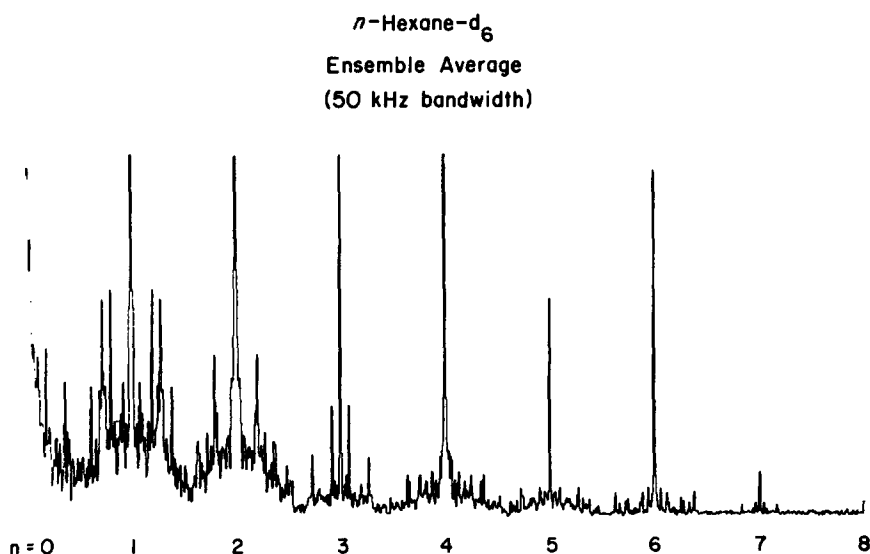
Ensemble Average

(50 kHz bandwidth)

Fig. 4. The proton multiple quantum spectra of oriented methyl-deuterated n-hexane obtained with the pulse sequence shown in fig. 1. Fifteen separate experiments were summed together to obtain the "ensemble averaged" multiple quantum spectrum.

tinct multiple quantum free induction decays (MQ FID) were obtained from preparation times varying from 2 to 14 ms. In each experiment, 4096 points were recorded in t_1 at intervals of 10 μs. For each point, twenty-eight transients were accumulated to improve signal to noise. Each MQ FID
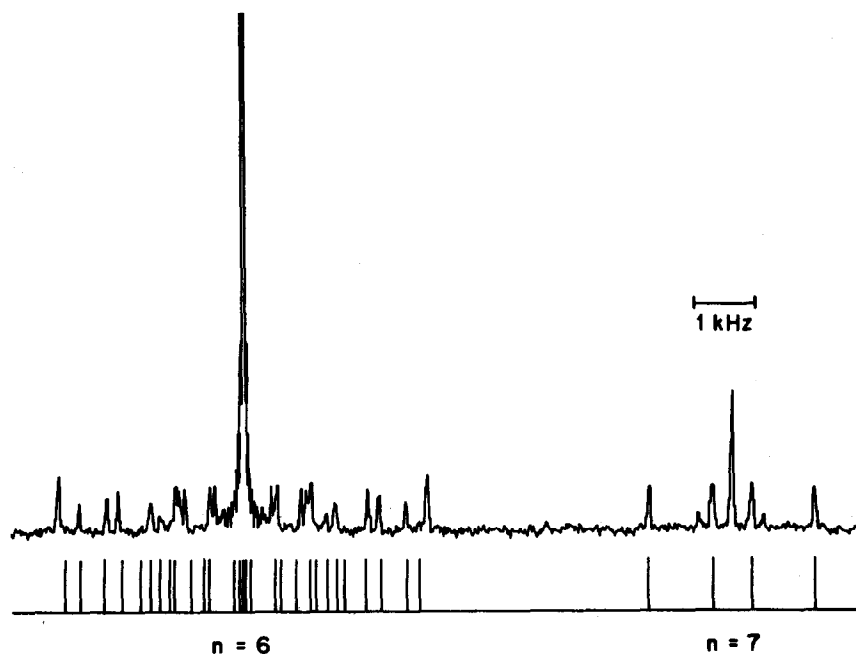

Fig. 5. Comparison of the experimental and calculated six-and seven-quantum spectra using the conformational probabilities noted in table 3 together with an S_{zz} value of 0.12.

was zero-filled to 8192, Fourier transformed, and the fifteen absolute magnitude spectra were then added together to yield the spectrum in fig. 4.

An expansion of the six- and seven-quantum regions is shown in fig. 5. The expectation of rapid motional averaging is confirmed by the appearance of only two pairs in the seven-quantum region. The central feature in this order is an artifact of a small pulse amplitude modulation which is concurrent with the TPPI cycle. The six-quantum region contains at least eleven resolved pairs and a highly degenerate central line, as expected. Simulations suggest that two pairs are unresolved from the central transition.

The noise is not independent on each side of the center of each order since the positive and negative frequency spectra resulting from TPPI have been shifted to a common center and added. The spectral resolution of 25 Hz is partially limited by data storage resulting in truncation of the interferogram in t_1 at the point where it had decayed to $\approx 1/e$.

2.3. Spectral simulation

There are ten independent proton–proton dipolar couplings in n-hexane-d_6, which is too few to attempt an exact inversion of eqs. (3) and (4). Eventually the present data set should be supplemented by ^{13}C–^1H couplings. Methods for such heteronuclear multiple quantum experiments have been discussed elsewhere [22]. Some preliminary spectral simulation is presented here to demonstrate the sensitivity of the spectra to different model assumptions and give some indication of the magnitudes involved.

The first simplifying assumption made is that the energy differences between the different allowed conformers are in proportion to the number of gauche bonds in each. The energy difference between the all-trans conformer and those with a single gauche is chosen such that the former is twice as probable as the latter. All conformers with adjacent gauche bonds are excluded, as these are considerably less linear than the others. With these assumptions the probabilities listed in table 3 result.

The next simplification is to assume that the

Table 3
Conformational probabilities for n-quantum simulation[a]

Configuration	Probability
ttt	0.2
tg$^\pm$t	0.1
ttg$^\pm$	0.1
g$^\pm$tt	0.1
g$^\pm$tg$^\pm$	0.05
g$^\pm$tg$^\mp$	0.05

[a] All other configurations probability = 0.

ordering is uniaxial, so that only $S_{zz}^n = C_{00}^{(2)}(\Omega_1^n)$ is finite, and that this has the same value for all configurations. The molecular z axis is normal to the H–C–H planes of the central methylenes except for the tg$^\pm$t configurations for which it lies along the central carbon–carbon bond. The bond distances are $r_{CC} = 1.54$ Å and $r_{CH} = 1.11$ Å. The bond angles are tetrahedral and the gauche minima are 120° away from the trans minimum.

The stick spectrum in fig. 5 shows the best fit to this model obtained by varying S_{zz}. A value of $S_{zz} = 0.12$ is found. No reasonable fit can be found for more restricted (e.g. pure ttt) conformational models. The rms error is 48 Hz which is equivalent to two digitized points. The dipolar coupling constants calculated from this model were used as the starting parameters in an iterative fitting program [23]. In this iteration, twenty-six $n = 5$ transitions were also included. Negligible improvement in the rms error resulted. In addition, the one-order-parameter model described above was also tested while allowing only the all-trans configuration or allowing all configurations except those containing the adjacent combination g$^\pm$g$^\mp$. Both of the resulting fits were considerably less satisfactory than that of fig. 5 and led to diverging iterations when used as starting parameters.

3. Discussion and conclusion

The MQ NMR spectra of oriented hexane-d_6 demonstrate the increased resolution as the number of quanta increases. The six- and seven-quantum spectra show the rapid conformational dynamics and a rough simulation is made using ttt,

tgt, ttg and gtg conformations of the chain. This forms a reasonable starting point for improvements on the current model with additional dipole couplings, for example using ^{13}C, and more vigorous fitting routines. Use of a high-resolution magnet or the TSCTES method [24,25] will remove any ambiguity about the role of chemical shifts, which are assumed here to be removed by the π pulse at $t_1/2$. This is only true to lowest order and should be checked, since a more exact analysis [26] shows that they can reappear as small line shifts and also introduce extra lines. With higher resolution data, inclusion of J couplings will also be necessary. Most importantly, additional dipolar and quadrupolar couplings should be measured on the same system.

We conclude that the use of high-order multiple quantum spectroscopy is a valuable tool for the study of non-rigid oriented molecules and n-hexane has been given as an example. The large number and geometric variety of the probes provided by proton dipolar couplings along with the possibility of resolving discrete transitions even in complex systems are distinct advantages over the deuterium or single quantum proton methods.

Acknowledgement

References

[1] J.W. Emsley and J.C. Lindon, NMR spectroscopy using liquid crystal solvents (Pergamon Press, New York, 1975).

[2] B. Deloche and J. Charvolin, J. Phys. (Paris) 37 (1976) 1497; 41 (1980) L 39.

[3] J. Seelig, Quart. Rev. Biophys. 10 (1977) 353.

[4] S. Hsi, H. Zimmermann and Z. Luz, J. Chem. Phys. 69 (1978) 4126.

[5] N. Boden, L.D. Clark, R.J. Bushby, J.W. Emsley, G.R. Luckhurst and C.P. Stockley, Mol. Phys. 42 (1981) 565.

[6] J.H. Davis, Biochim. Biophys. Acta 737 (1983) 117.

[7] E.T. Samulski and R.Y. Dong, J. Chem. Phys. 77 (1982) 5070.

[8] P.J. Flory, Statistical mechanics of chain molecules (Wiley–Interscience, New York, 1969).

[9] J.W. Emsley and G.R. Luckhurst, Mol. Phys. 41 (1980) 19.

[10] J.W. Emsley, G.R. Luckhurst and C.P. Stockley, Proc. Roy. Soc. A381 (1982) 117.

[11] G. Drobny, Ph. D. Thesis, University of California, USA (1982).

[12] E.E. Burnell and C.A. De Lange, J. Magn. Reson. 39 (1980) 461.

[13] A. Saupe, Z. Naturforsch. A 19 (1964) 161.

[14] P. Diehl, Pure Appl. Chem. 32 (1972) 111.

[15] A. Pines, D. Wemmer, J. Tang and S. Sinton, Bull. Am. Phys. Soc. 21 (1978) 23.

[16] G. Drobny, A. Pines, S. Sinton, D.P. Weitekamp and D. Wemmer, Faraday Symp. Chem. Soc. Symp. 13 (1979) 49.

[17] J. Tang and A. Pines, J. Chem. Phys. 73 (1980) 2512.

[18] S. Sinton and A. Pines, Chem. Phys. Letters 76 (1980) 263.

[19] G. Bodenhausen, Proc. Nucl. Magn. Reson. Spectry. 14 (1981) 137.

[20] D.P. Weitekamp, Advan. Magn. Reson. 11 (1983) 111.

[21] E. Hahn, Phys. Rev. 80 (1950) 580.

[22] D.P. Weitekamp, J.R. Garbow and A. Pines, J. Chem. Phys. 77 (1982) 2870.

[23] J.B. Murdoch, Ph. D. Thesis, University of California, USA (1982).

[24] D.P. Weitekamp, J.R. Garbow, J.B. Murdoch and A. Pines, J. Am. Chem. Soc. 103 (1981) 3578.

[25] J.R. Garbow, D.P. Weitekamp and A. Pines, J. Chem. Phys. 79 (1983) 5301.

[26] M.A. Thomas and A. Kumar, J. Magn. Reson. 47 (1982) 535.